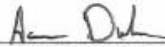


Optimization of the WPI Kite-Powered Water Pump

A Major Qualifying Project Report
Submitted to the Faculty of the
WORCESTER POLYTECHNIC INSTITUTE
in Partial Fulfillment of the Requirements for the
Degree of Bachelor of Science
in Aerospace Engineering

by



Aaron Durkee



Christopher Ettis



Dong Hae Kim



David Levien

May 1, 2014

Approved by:



Professor David Olinger, Advisor
Aerospace Engineering Program
Aerospace Engineering Department, WPI

Abstract

This project furthers the design and testing of the WPI kite-powered water-pump system. The purpose is to provide developing nations with an inexpensive airborne wind energy system capable of efficiently and consistently pumping water. After initial field testing in fall 2013, several design modifications were made. These included developing improved kite stall techniques, a mobile trailer system, and designing and building an automated water-pumping volume measurement system. The trailer allows for field testing of a wider range of locations. Modifications were successfully field tested in spring 2014. An existing MATLAB simulation was also modified to model random wind variations.

“Certain materials are included under the fair use exemption of the U.S. Copyright Law and have been prepared according to the fair use guidelines and are restricted from further use.”

Acknowledgements

We would like to thank the following individuals and groups for their help and support throughout the entirety of this project.

Project Advisor Professor David Olinger

Heifer Farm, Rutland MA Shon Rainford

Blue Hill Observatory &
Science Center Don McCasland

Table of Authorship

Section	Author(s)
<i>Background</i>	
1.1	CE, DHK
1.2, 1.3	AD
1.4, 1.5	DL
<i>Methodology</i>	
2.1, 2.3, 2.4	DL, DHK
2.5	CE
2.6	AD
<i>Results</i>	
3.1	AD
3.2	CE
<i>Summary and Conclusions</i>	AD, DL
<i>Recommendations and Further Work</i>	
5.1, 5.4	DL
5.2, 5.5	AD
5.3	DL, DHK
<i>Appendix A</i>	AD

Key: AD=Aaron Durkee, CE=Christopher Ettis, DHK= Dong Hae Kim, DL= David Levien

Table of Contents

Abstract.....	1
Acknowledgements.....	2
Table of Authorship	3
Table of Contents.....	4
List of Figures	7
List of Tables	9
1.0 Background	10
1.1 Airborne Wind Energy.....	10
1.1.1 Airborne Wind Energy.....	10
1.1.2 WPI Kite Powered Water Pump System	11
1.1.3 Advantages and Disadvantages	12
1.1.4 Optimization of AWE Systems	13
1.2 Location Testing.....	13
1.3 Relation to Undeveloped Nations.....	14
1.4 Previous MQP Results	15
1.5 Project Goals	17
2.0 Methodology.....	18
2.1 Design Processes.....	18
2.2 Instrumentation	20
2.2.1 Inclinator	20
2.2.2 Load Cell.....	20
2.2.3 Amplifier.....	21
2.2.4 DAQ.....	21
2.2.5 LabVIEW	22

2.2.6 Wind Sensor	22
2.2.7 Well Depth Simulator.....	23
2.3 Field Testing	24
2.3.1 Instrumentation	24
2.3.2 Kite	24
2.4 Water-pump System Trailer Modifications.....	25
2.4.1 Water-dumping Mechanism	26
2.5 MATLAB Simulation.....	29
2.6 Project Website.....	29
3.0 Results.....	31
3.1 Field Testing	31
3.2 MATLAB Simulation	33
4.0 Summary and Conclusions	36
5.0 Recommendations and Future Work.....	37
5.1 Trailer Field Testing.....	37
5.2 Leading Edge Stall Recovery System	37
5.3 Kite Auto-Launch.....	37
5.4 Website Updates.....	38
5.5 Instrumentation Housing	38
6.0 References	39
Appendix A. Instrumentation Manual	40
Load Cell.....	40
Inclinometer.....	40
Battery.....	41
Amplifier.....	41

DAQ..... 43

Wiring Overview Table..... 45

LabVIEW Virtual Instrument 45

List of Figures

Figure 1 - Simple spooling line concept (1-Kite, 2, Tether, 3- Spool, 4-Gearbox and motor, 5-Generator, 6-Kite steering mechanism, 7-Crosswind kite motion) (Olinger, 2010).....	11
Figure 2 - Diagram of this project's water-pump system (Olinger et al. 2013)	12
Figure 3 - Heifer Average Monthly Wind Speed at 50m (m/s) from 9/17/2007 to 8/8/2008 (Chretien)...	14
Figure 4 - Annual mean wind speed in Southern Africa, 50m a.s.l. in 2005 (NASA SSE 2005).	15
Figure 5 – Method 1, Water-pump system in the new trailing-edge to ground configuration.....	18
Figure 6 – Method 2, Water-pump system in the new pulley system configuration	19
Figure 7 – Method 3, Water-pump system in the new leading-edge stall configuration.....	19
Figure 8 - Rieker N4 Liquid Capacitive Electronic Analog Output Inclinometer Sensor and Specifications	20
Figure 9 - Transducer Techniques THB-1K-S and Specifications.....	20
Figure 10 – Amplifier and Specifications.....	21
Figure 11 – National Instruments DAQ and Specifications	21
Figure 12 - Oregon Scientific Weather Station in the Lab	22
Figure 13 - The pressure pump (right) and its location on the water-pump system (left).....	23
Figure 14 - The spring and rod within the pressure simulator pipe	23
Figure 15 - The Lark's Head knot used to tie the tethers to kite lines and to the water-pump system (http://www.kiteboardingevolution.com/larks-head-knot.html)	24
Figure 16 - Raised A-frame structure.....	25
Figure 17 - Extended and raised water-pump piping	25
Figure 18 - Wooden support beam to be raised.....	26
Figure 19 – Inside of the tipping bucket mechanism.....	27
Figure 20 - The weight underneath the tipping bucket.....	27
Figure 21 - Completed tipping bucket mechanism.....	28
Figure 22 - Automatic-counter mechanism	28
Figure 23- Screenshot of the Welcome Screen on the Project Website	30

Figure 24 - Power Spectral Density of Horizontal Wind Speed (Van der Hoven, 1956)	33
Figure 25 - Simulation Performance Parameters on a 20 Second Interval.....	34
Figure 26 - Simulated Power Generation on a 20 Second Interval.....	35
Figure 27 - Auto-launch concept design	37
Figure 28- Wiring Diagram for THB-1K-S Load Cell (Transducer Techniques)	40
Figure 29- Inclinometer Extension Wiring	41
Figure 30- Battery Wired to Amplifier	41
Figure 31- Amplifier Wiring Diagram	42
Figure 32- Load Cell Wired into Amplifier.....	42
Figure 33- Power and Signal Output Wired from Amplifier.....	43
Figure 34- DAQ Wiring	44
Figure 35- Sample Device/Channel Input for LabVIEW VI	46
Figure 36- Inclinometer Calibration Tools	46
Figure 37- Load Cell Calibration Tools.....	47

List of Tables

Table 1 - Previous MQP Results (Butler, 2013)	15
Table 2- Pulley Configuration Test Data	32
Table 3 - Wiring Overview.....	45

1.0 Background

A wind-powered water pump has the potential to drastically improve the quality of life in developing nations by making a vital resource more easily attained. This project addresses the need for a simple, reliable, and consistent solution to the water needs of emerging lands.

One of the most basic and reliable methods of pumping water is the manual hand-pump. A hand-pump is simple and effective; however, it requires a lot of time and effort. Hand pumps will only produce water for as long as a person is willing to operate them, which is not an effective means of producing large quantities. Other methods of more efficient operation must be considered in order to run the water pump autonomously and for long periods of time. One such alternative and more efficient method is airborne wind energy systems.

The primary method of utilizing airborne wind energy discussed in this project is kites or rigid gliders. With their simple operation and maintenance, kites are a cost-effective and energy-effective method of harnessing wind for the purpose of operating a water pump. Compared to conventional windmills, kites are able to reach stronger winds at higher altitudes and have less of an environmental disturbance while remaining relatively inexpensive. Wind farms are often inefficient in land utilization, as well, while kites do not require large towers and foundations. This project aims to improve upon the research and kite-system created by past project teams by increasing the efficiency.

1.1 Airborne Wind Energy

Airborne Wind Energy (AWE) is a type of renewable energy using wind and kites or rigid gliders to generate power. AWE systems, first proposed and studied by Loyd in 1980, have been designed for human resources such as transportation of sea or land vehicles, water pumping, and electricity generation (Loyd, 1980). Generally, the use of AWE is widely accessible in areas of medium and high altitude where wind can be most easily captured. AWE systems have a relatively low production cost and have the potential to produce significant power. Most current AWE systems with significant power output need to be tethered to the ground in order to generate energy (Diehl, 2013).

1.1.1 Airborne Wind Energy

Airborne wind energy research uses two distinct methods of power generation: FlyGen and GroundGen. In FlyGen, power from drag forces is generated in airborne turbines by the high airspeed relative to the tethered wing. In GroundGen power from lift is utilized by pulling a load on the ground using tether tension (Diehl, 2013). This project's kite system generates power using lift. An advantage to using lift is the simplicity of implementation; the mechanical system that generates energy does not need to be light enough to fly with the kite. Tension in the tether of a flying kite will always have a vertical force component, which is ideal for lifting the lever-arm of a pump on the ground (Diehl, 2013).

Tether tension becomes useful by performing work on the ground, in this case by operating the lever-arm of a water pump. Lever-arm displacement is accomplished by the looping motion of the kite flying in a crosswind, varying the tether tension strength and direction. For this project's system, the desired variation in tension is caused by the repeated stalling of the kite at a specific angle of attack gained from the control of the leading and trailing edge tethers. With the goal of improving water pump efficiency at

various wind speeds, field experimentation is designed to investigate the relationship of tether tension, angle of attack, and their control method.

Figure 1, below, demonstrates the majority of the concepts discussed above using a simple spooling line concept. A mechanism on the ground is attached to a kite in the air using a tether. The rising kite generates power followed by a retracting stroke to repeat the process. Though this project uses a rocking arm rather than a spool, the same principle generates power to lift and lower the water pump piston.

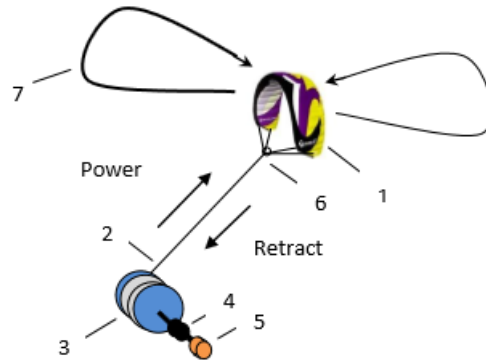


Figure 1 - Simple spooling line concept (1-Kite, 2, Tether, 3- Spool, 4-Gearbox and motor, 5-Generator, 6-Kite steering mechanism, 7-Crosswind kite motion) (Olinger, 2010).

1.1.2 WPI Kite Powered Water Pump System

The system to be tested and re-designed by this project team was constructed by previous WPI MQP teams and is shown in Figure 1. The system consists of a grounded A-frame (2) supporting a 134 inches rocking arm (1) at a pivot point (B) 89 inches from the end (point A) where the kite tether is attached. This rocking arm is attached by a mechanical linkage (b) to the displacement water pump at point C. The rocking arm is lifted by the tension in the main kite tether at point A, and is caused to drop by decreasing this lift using various control methods that are described further in the Methodology section. Each control method involves an additional tether to which tension is applied at the time of maximum rocking arm inclination. The rocking motion of the arm is transferred to the displacement pump by the mechanical linkage. A one-way valve (10) on the piston of the water pump opens on the down-stroke, allowing the system to return to its initial configuration (Bartosik et al., 2012; Butler et al., 2013).

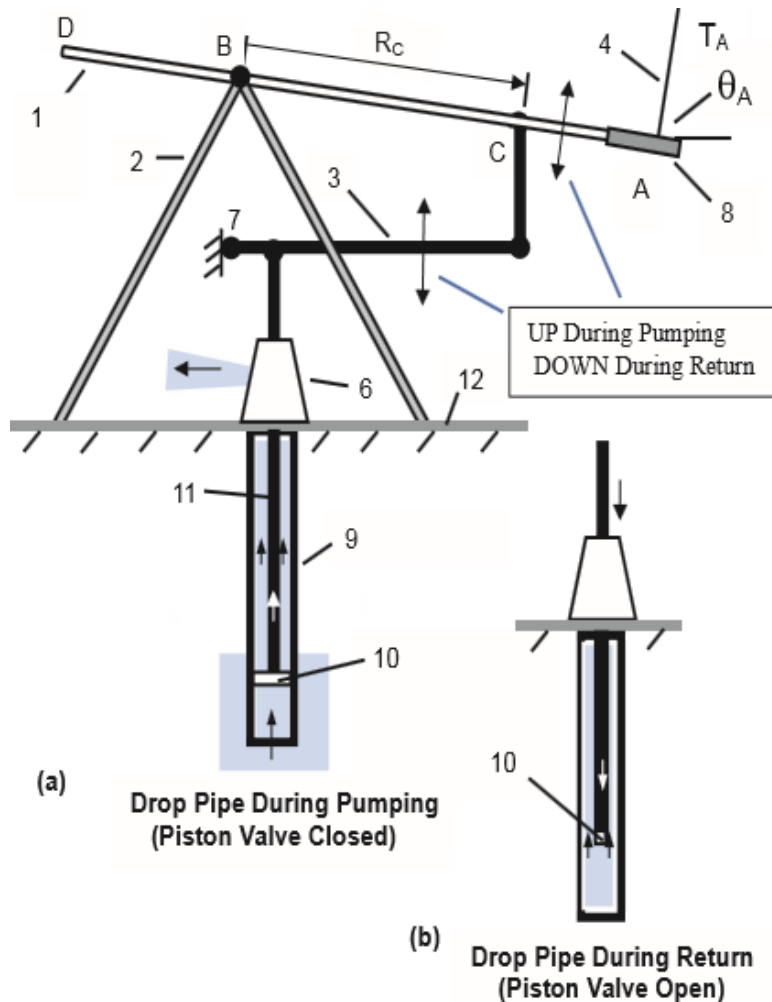


Figure 2 - Diagram of this project's water-pump system (Olinger et al. 2013)

In addition to previous field testing, WPI researchers have evaluated the feasibility of the kite power system using mathematical models. This project's experimentation aims to examine the performance parameters of the kite power system, and to modify the design to more closely approximate the ideal numerical predictions simulated in previous work on our projects system (Olinger et al, 2013). The current model (Olinger et al., 2013) optimized dimensions of the tethers and determined that with a constant wind speed of 6 meters per second, 8000 liters of water pumped per day is predicted.

1.1.3 Advantages and Disadvantages

This project's research concentrates on the kite-powered water pump system that uses a cycle of increasing lift and stalling of the kite to move a rocking arm that is linked to the water pump's handle. There are three major reasons for the increasing interest in AWE for alternative energy. The first reason is that wind energy is one of the few alternative energy sources abundant enough to satisfy the power needs of humans. As long as a location has a sufficient level of wind, AWE systems may be installed and operated. Second AWE systems are able to reach higher altitudes than towered wind turbines, where

wind is stronger. AWE systems also have with simpler designs, and can be removed and reinstalled more quickly and inexpensively than towered-wind turbines. Lastly, AWE systems require less material investment per unit of usable power output than most other renewable energy sources, meaning that these systems produce energy at a lower cost.

AWE systems also have disadvantages. Wind dependency may be considered one of the most significant disadvantages of the kite-powered systems. Changing wind directions and slow wind speeds may stall the airfoil, creating the possibility for a tethered wing to crash. Theoretical calculations using optimal operational wind speeds versus power output also show that two-thirds of the wind's power is dissipated in forms of drag and only one-third produces reliable energy. Lastly, the intrinsic drag due to the tether line that affects the lift-drag ratio $\frac{C_L}{C_D}$ enters the limit quadratically. Since kites with more lift produce more energy, a lower drag coefficient is desired. In the case of kite-powered systems, the tether drag becomes a dominant drag contribution.

1.1.4 Optimization of AWE Systems

Optimizing AWE systems mean overcoming the technical challenges. Technical challenges for AWE systems include:

- Developing low-cost, automated methods of launching and landing
- Developing efficient autonomous control of the kite under all wind and weather conditions
- Designing wings or frames that are light and durable enough for the system
- Finding or developing tethers with thinner diameter but capable of varying load, as well as capable of transmitting high voltage electrical power for on-board generation

Optimization relies on calculations and estimations based on the most economical and efficient sizes of the airborne system. Solving for the amount of wind power that can be generated on a given ground surface area is also important for optimization. According to MacKay(2009), conventional wind turbine farms produce 2 megawatts (MW) per square kilometer (km²), which is considered less efficient than with airborne wind energy systems (MacKay, 2009). As previously stated, airborne wind energy systems can reach higher altitudes with stronger and more consistent winds, and may also operate at more than one level in order to maximize the power output over a given ground surface area.

1.2 Location Testing

The current location for the kite powered water pump is Heifer Farm in Rutland, MA. Heifer Farm's mission is "To work with communities to end hunger and poverty and care for the Earth" (Chretien, 2008). The farm hosts events that reach out to the community to teach others about sustainable living, agriculture, and the needs of undeveloped nations. The Heifer organization views the kite-powered water pump as an aspect of their mission and has granted the use of their land for testing purposes.

In 2006, Heifer Farms worked with Mass Energy to explore the feasibility of erecting a wind turbine at Overlook Farm. Jeff Collins of Mass Audubon provided an environmental impact analysis, while

Lighthouse Electrical installed the MET tower to collect data and provided site visualizations and simulations. Financial analysis was conducted by Michele Bilodeau, the Fiscal Director of Mass Energy. Mass Energy compiled data, provided a final report to determine feasibility, and concluded that at the time of the report a wind turbine was not economically feasible. This final report also provides monthly wind speed averages above ground level that are useful for simulations for the kite power project.

Heifer Average Monthly Wind Speeds

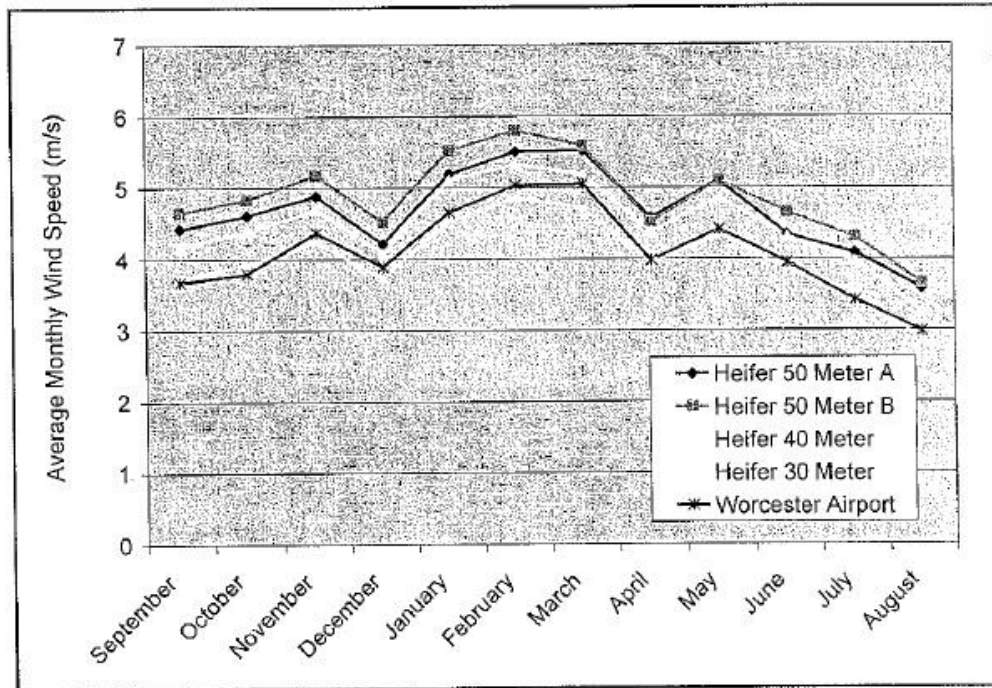


Figure 3 - Heifer Average Monthly Wind Speed at 50m (m/s) from 9/17/2007 to 8/8/2008 (Chretien).

1.3 Relation to Undeveloped Nations

The kite-powered water pump has the potential to make a powerful impact in undeveloped nations where clean water is scarce, such as Africa. An approximate wind speed of 10 miles per hour (4.4 meters per second) is required to lift and maintain the kite's flight. The following map shows averaged wind speeds at 10 meters above ground level across Africa from 1976 through 1995.

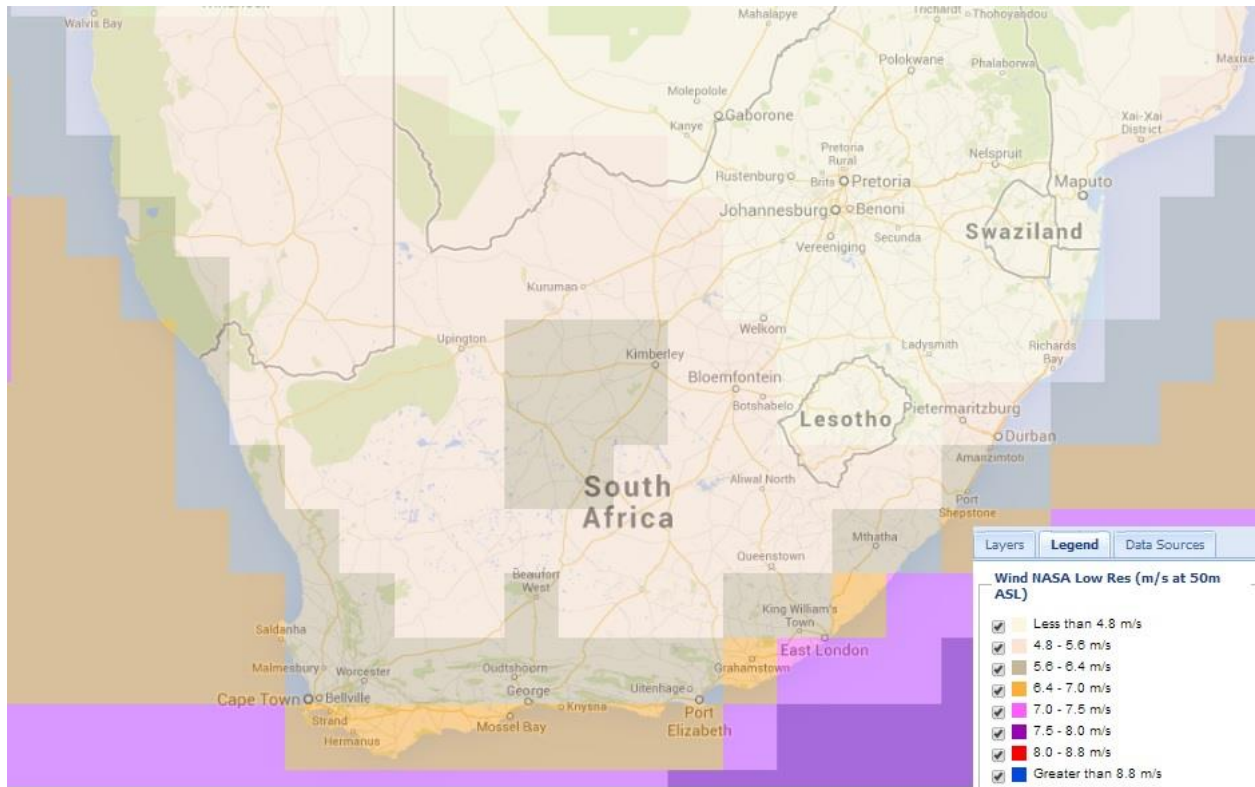


Figure 4 - Annual mean wind speed in Southern Africa, 50m a.s.l. in 2005 (NASA SSE 2005).

Regional wind speeds are important for the operation of the kite system. As height above ground level increases, so does average wind speed. An average wind speed within the range of the kite’s required launch speed makes it possible to launch the kite; therefore, kite-powered water pumps are likely able to be attached to existing water pumps throughout much of Southern Africa, as well as other undeveloped nations. A possible country for use of the kite powered water pump is Namibia on the Southwestern coast of Africa. WPI maintains a project center in Windhoek, Namibia.

1.4 Previous MQP Results

The progress of this project builds upon the accomplishments of previous WPI MQP students. Key details of projects from past years, including this year’s project, are listed below in Table 1.

Table 1 - Previous MQP Results (Butler, 2013)

Year	IQP/MQP Title	Students	Main Accomplishments
2007	Wind Power From Kites MQP	Michael R. Blouin Jr. Benjamin E. Isabella Joshua E. Rodde	Designed and constructed the basic A - frame structure and rocking arm. Selected kite for use in power generation based on testing and mathematical analysis. Ran simulations based on steady state and dynamic theory of the tested kites.
2008	Kite Power for Heifer International’s	Gabriel Baldwin Peter Bertoli Taylor LaLonde	Developed educational exhibits on kite power for use at the Heifer International's Overlook Farm site.

	Overlook Farm IQP	Michael Sangermano Nick Urko	
2008	Design of a One Kilowatt Scale Kite Power System MQP	Ryan Buckley Chris Colschen Michael DeCuir Max Hurgin Erik Lovejo Nick Simone	Completed and tested the demonstrator which was able to generate power as well as autonomously keep the kite aloft for a short period of time. Performed stress analysis in Cosmosworks and ran power generation simulations in MATLAB.
2009	Development of a Wind Monitoring System and Grain Grinder IQP	Deepa Krishnaswamy Joseph Phaneuf Travis Perullo	Designed a balloon mounted wind monitoring system using an anemometer. Implemented a small grain grinder to be attached to the power converter on the kite power system.
2009	Design of a Data Acquisition System for a Kite Power Demonstrator MQP	Lauren Alex Eric DeStefano Luke Fekete Scott Gary	Designed data collection system for physical attributes of the system as well as for power generation. Designed secondary power generation and oscillation control subcomponents. Further optimized rocking arm and A-frame as well as tested each system and subcomponent.
2010	Design of a Dynamometer For The WPI Kite Power System MQP	C. Kuthan Toydemir	Designed and built a dynamometer used to measure torque and power.
2010	Re-Design and Testing of the WPI Kite Power System MQP	Adam Cartier Eric Murphy Travis Perullo Matthew Tomasko Kimberly White	Modified system: Used a more stable and larger sled kite Upgraded gear shaft Built mechanism to change angle of attack of kite Measured tension of kite tether during testing
2011	Design of a Remote Controlled Tether System for the WPI Kite Power System MQP	Michael Frewin Emanuel Jimenez Michael Roth	Developed wireless system to remotely control trailing edge lines of kite to alter angle of attack and side-to-side motion Designed a control box with two motors, gear boxes, transmitters, and two spools to control the length of trailing tethers.
2012	Design of a Kite-Powered Water Pump and Airborne Wind Turbine MQP	Kyle Bartosik Jennifer Gill Andrew Lybarger Daniel Nyren John Wilde	Redesigned system to add a mechanical water pump and head simulation valve
2013	Re- Design of the WPI Kite-Powered Water Pump and Wind Turbine Systems	Valerie Butler Jeffrey Corado Kimberly Joback Bryan Karsky Matthew Melia	Altered transfer arm Modified sliding weight mechanism Added adjustable weight to rocking arm Added a ground-tether Redesigned lightweight, airborne wind turbine

		Robert Monteith Brandy Warner	
2014	Optimization of the WPI Kite Powered Water Pump	Aaron Durkee Chrisopher Ettis Jerry Kim David Levien	Performed extensive field testing on the kite system Created a functioning VI in LabVIEW for data acquisition Created a simulation using MatLab to model random wind speeds Design a portable trailer system

1.5 Project Goals

The overall aim of this project was to improve the WPI kite-powered water pump. Specific project goals are:

- Perform further field testing on the kite system to gather data including tether tension, arm angle, and water pumping rates
- To create a functioning VI in LabVIEW to gather data from testing instrumentation
- Propose mechanical modifications to further improve the function of the water pump and power generation system based on the measured data
- To modify an existing simulation of the water pump to model wind gusts and random wind conditions using MATLAB
- To improve kite stalling mechanisms on the system
- To design a portable trailer system and automated pumping volume measurement system in order to transport the water pump and improve field testing

These goals were chosen based on the progress and results of previous MQP projects. The experimental methods used to accomplish these goals are described in the following section.

2.0 Methodology

2.1 Design Processes

Multiple configurations of kite-pump system have been developed in this year's project using the mechanical system established in previous projects. The various setups are all attempts to optimize the overall operation of the system to reliably pump water by varying the method of stalling the kite with different tether configurations (shown in Figures 4-6).

In the first configuration (method 1) a bridle tether is attached between the kite leading edge and rocking arm while the stalling tether is attached between the trailing edge and the ground.

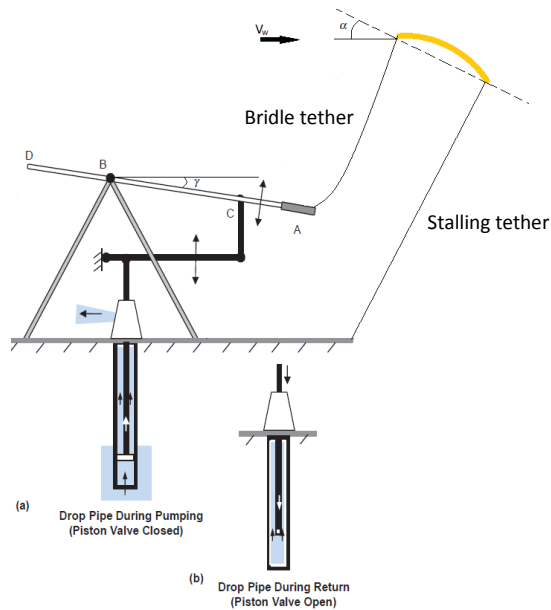


Figure 5 – Method 1, Water-pump system in the new trailing-edge to ground configuration

When the kite is lifted, the bridle tether pulls the lever-arm up. The rising kite then reaches a point where tension in the grounded stalling tether allows only the leading edge of the kite to rise to a stalling angle of attack, causing the kite to fall. The decreased lift and the weight of the arm then pull the kite back down, lowering the lever-arm to start a new pump cycle.

In the second configuration (method 2) is the pulley system, consisting of a grounded pulley that connects the stalling tether to the rocking arm.

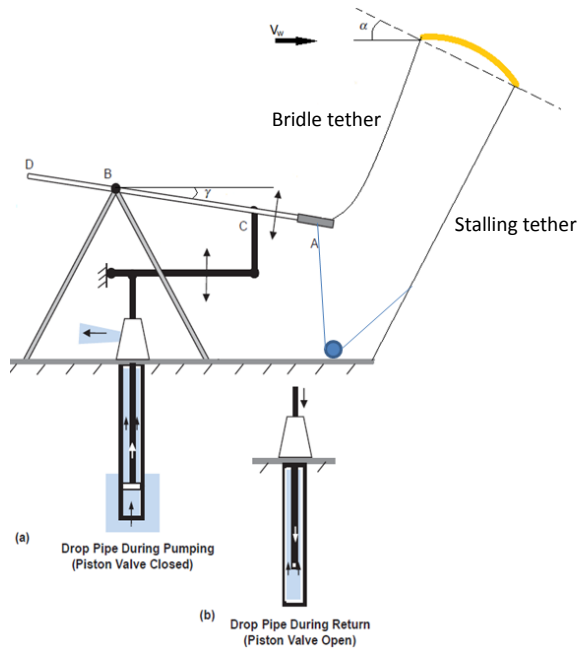


Figure 6 – Method 2, Water-pump system in the new pulley system configuration

The pulley-system helps to stall the kite by allowing the lifting of the rocking arm to also pull down on the kite's trailing edge.

The new, third configuration (method 3) required modifications to an existing kite. An additional leading edge tether was stitched to the upper corners of the kite's central stabilizing flow tube, while the trailing edge tether was removed completely.

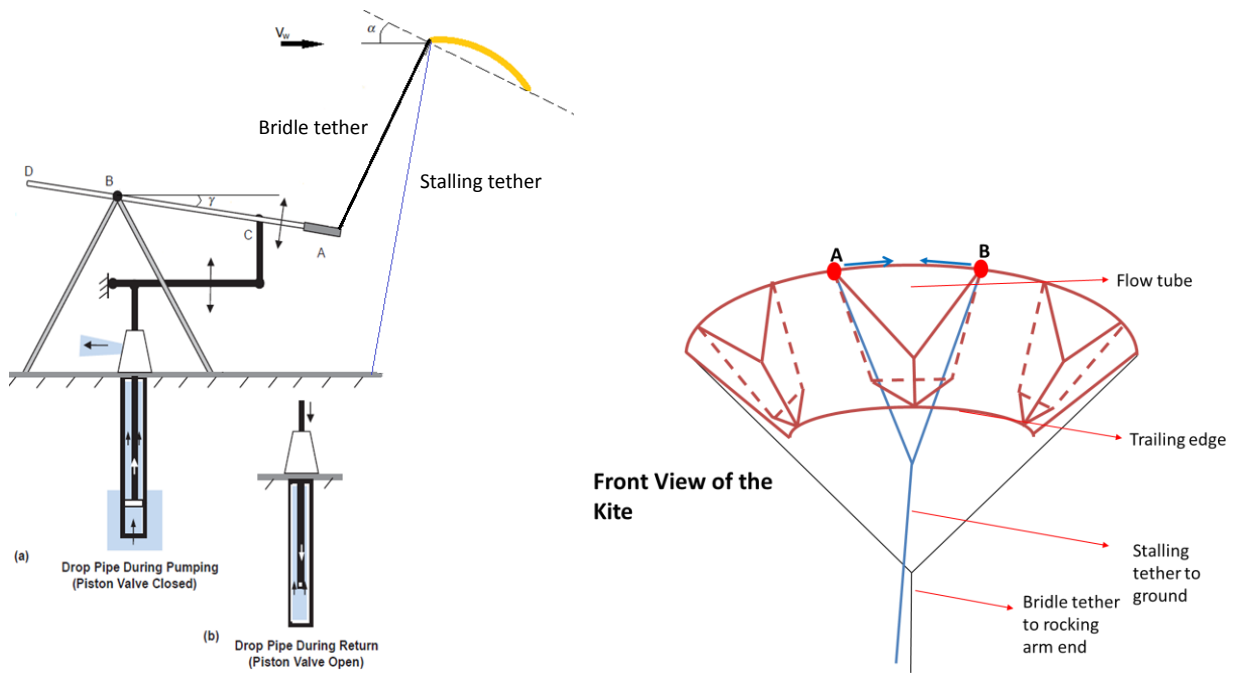


Figure 7 – Method 3, Water-pump system in the new leading-edge stall configuration

This setup closes the center tube of the kite when tension is placed on the stalling tether to prevent flow through the stabilizing tube when the center of leading edge is pulled, causing the kite to become unstable, lose altitude, lower its angle of attack, and drop the lever-arm. Once the tension in the stall line is released, the kite center tube is reopened regaining airfoil shape and stability to once again experience a lift force, thereby lifting the lever-arm.

2.2 Instrumentation

Instrumentation and software were used to measure forces, angles, and wind speed during field testing of the WPI kite-powered water-pump. This data could later be used to deduce the effectiveness of different configurations as well as any other changes in performance. The following hardware was all supplied for this project, with the goal being to refine and improve the data acquisition system.

2.2.1 Inclinometer

Rieker N4 Liquid Capacitive Electronic Analog Output Inclinometer Sensor



Range	-70° to 70°
Resolution	0.01°
Power Supply	5 VDC

Figure 8 - Rieker N4 Liquid Capacitive Electronic Analog Output Inclinometer Sensor and Specifications

The inclinometer is mounted on the rocking arm and used record the angle of the lever-arm. Angles are measured from the horizontal and over a chosen time interval. Data collected shows the periodic motion of the lever-arm, and therefore also water-pump lever, allowing for the quantitative observation of oscillations and the angle at key points in the pump cycle, such as the lifting stage and stall point.

2.2.2 Load Cell

Transducer Techniques THB-1K-S



Capacity Range	1000 lbs
Rated Output	2 mV/V nominal
Excitation Voltage	10 VDC

Figure 9 - Transducer Techniques THB-1K-S and Specifications

The load cell is compressed by its housing bracket due to the tension between the kite-tether and lever-arm. Data collected by the load cell shows the force that the kite is exerting on the lever-arm at various points throughout the pump cycle. Key points of the pump cycle such as the lifting stage and especially the stall point are important to gain an understanding of the effectiveness of each kite system configuration.

2.2.3 Amplifier

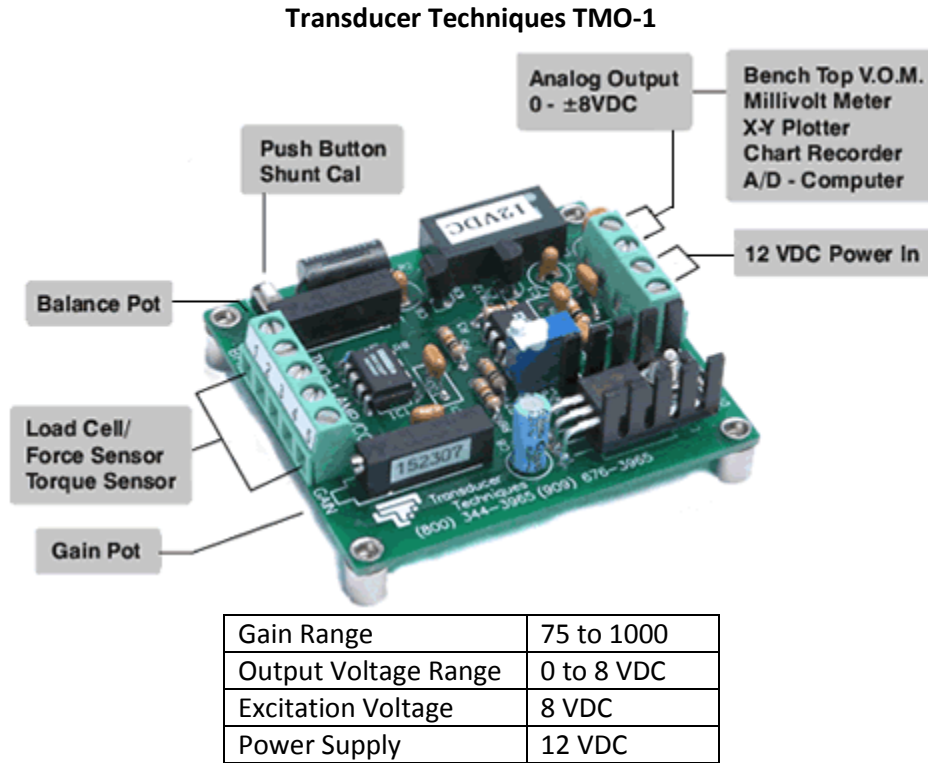


Figure 10 – Amplifier and Specifications

The amplifier is used to provide excitation voltage to the load cell, and to amplify the load cells output signal to levels that can be read by the DAQ.

2.2.4 DAQ

National Instruments USB-6000



Figure 11 – National Instruments DAQ and Specifications

The National Instruments Data Acquisition (DAQ) reads the voltages from the inclinometer and the load cell, and then sends that information into the LabVIEW VI via USB. The DAQ also provides the 5V power supply for the inclinometer sent from the LabVIEW via USB.

2.2.5 LabVIEW

The virtual instrument (VI) constructed in LabVIEW is used to calibrate the inclinometer and load cell to output measurements in appropriate units, display the measurements on charts, and to record the measurements in a Microsoft Excel file. The VI is controlled on a front panel that feeds parameters to the block diagram. Controls include switches for automatic inclinometer calibration, for writing to an Excel sheet, and for selecting the file path of that Excel sheet. The data displayed by the VI includes the instantaneous angle read by the inclinometer, force on the load cell, and the graphs of these values versus time.

2.2.6 Wind Sensor

The Oregon Scientific WMR200A is a home weather station capable of recording and displaying the temperature around the display unit, the weather station temperature, barometric pressure, rainfall, humidity, wind speed, and wind direction. This project used the unit primarily to determine wind speed and direction, as this data could be used in the force equations for the kite system.

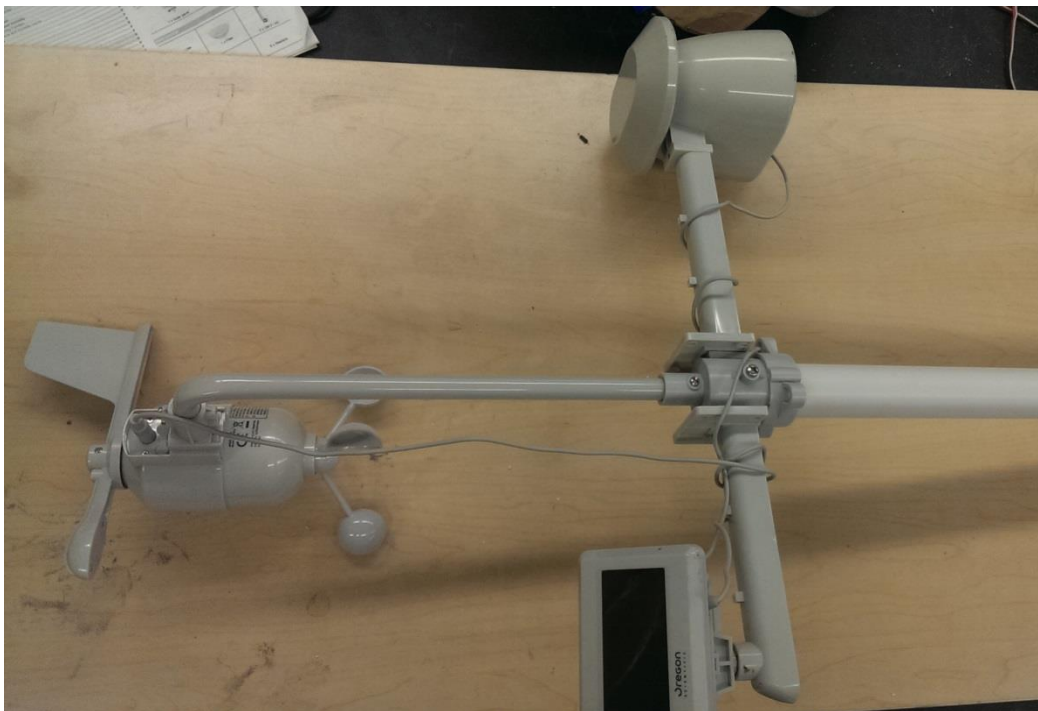


Figure 12 - Oregon Scientific Weather Station in the Lab

A trial version of Virtual Weather Station by Ambient Weather was used to read the values recorded by the WMR200A. This program provided a near real-time display of incoming data, which is the reason it was chosen over the WMR200A's one minute recording intervals. The program was set to save the speed and direction of the wind and of gusts over a one minute time interval to a Microsoft Excel file. The images providing more frequent updates were able to be saved manually, as the program did not provide an efficient method of doing so.

2.2.7 Well Depth Simulator

Water wells vary in depth, meaning that they also vary in the force necessary to pump out their water. The pressure, or well-depth, simulator was used to mimic the cases of deeper wells by increasing the force needed to pump the water.

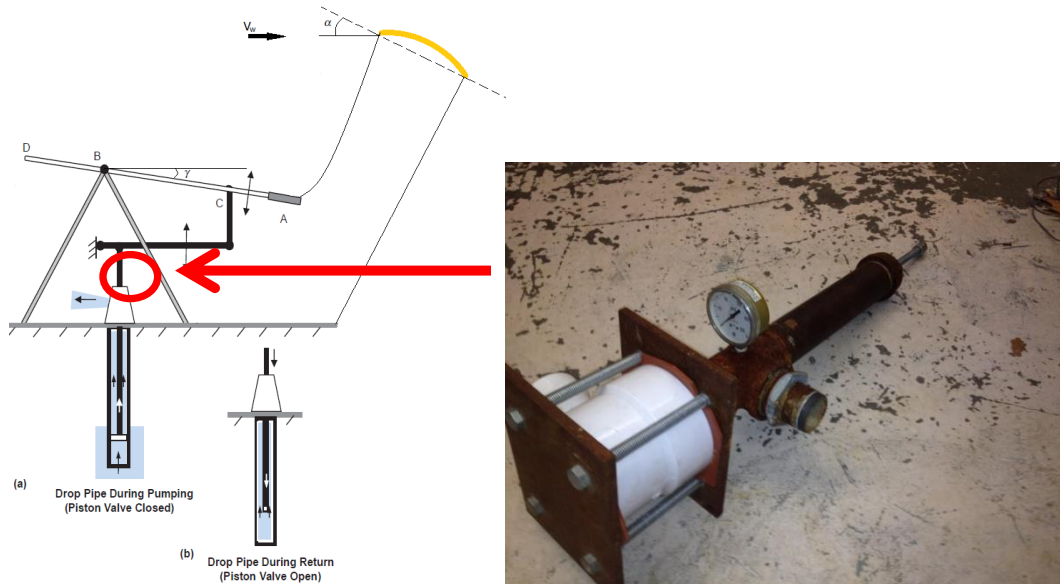


Figure 13 - The pressure pump (right) and its location on the water-pump system (left)

The pressure simulator works by changing the area of the orifice that the water is being pumped through, thereby changing the water pressure. As the rod protruding from the end of the pipe is turned counterclockwise, it screws out of the pipe and pulls on a spring (pictured below). As the spring is extended it pulls on a rod that reduces the orifice out of which the water flows; so, the more that the spring is extended the higher the water pressure will be, resulting in the simulation of a deeper well.



Figure 14 - The spring and rod within the pressure simulator pipe

2.3 Field Testing

The primary goal of this project is to gather data through field testing the water-pump system and its different configurations. Field testing encompasses the use of all instrumentation, kites, and the previously built structure.

2.3.1 Instrumentation

In order to gather data while field testing each piece of instrumentation must be attached to the water-pump system. The following are steps to set up instrumentation:

1. Secure the DAQ and amplifier under the leg of the system using Velcro
2. Attach the load cell to the eye-hook at the end of the lever-arm so that it is between the kite-tether and the lever-arm
3. Secure the inclinometer at its zero position to the mount on the side of the lever-arm
4. Plug the DAQ in to the laptop
5. Open the corresponding the LabVIEW program

In addition to these steps, the wind sensor must be turned on and have the year, date, and time set correctly. Once all of the instrumentation is set up and running, the system is ready to gather data.

2.3.2 Kite

Before there is any data to be gathered, the kite must be unpacked and attached to the water-pump system and instrumentation. The kite is set up using the following steps:

1. Unwind the tethers, starting from the water-pump system and moving outwards
2. Unpack the kite, including untying and untangling all lines, and lay it on the ground (if the wind is strong, put a weighted item on top of the kite to prevent it from blowing away)
3. Tie the tethers to the corresponding kite lines using the Lark's Head knot (corresponding tethers and lines depends on the chosen configuration)



Figure 15 - The Lark's Head knot used to tie the tethers to kite lines and to the water-pump system (<http://www.kiteboardingevolution.com/larks-head-knot.html>)

Once the above steps are completed, all of the tethers and instrumentation are secure and the kite may be launched.

2.4 Water-pump System Trailer Modifications

In order for the water-pump system to be more easily tested, it was modified so that it may operate on a trailer and be transported to various locations. The steps for modification are listed below:

- Raised the A-frame off of the ground in order for a water reservoir to be kept underneath.

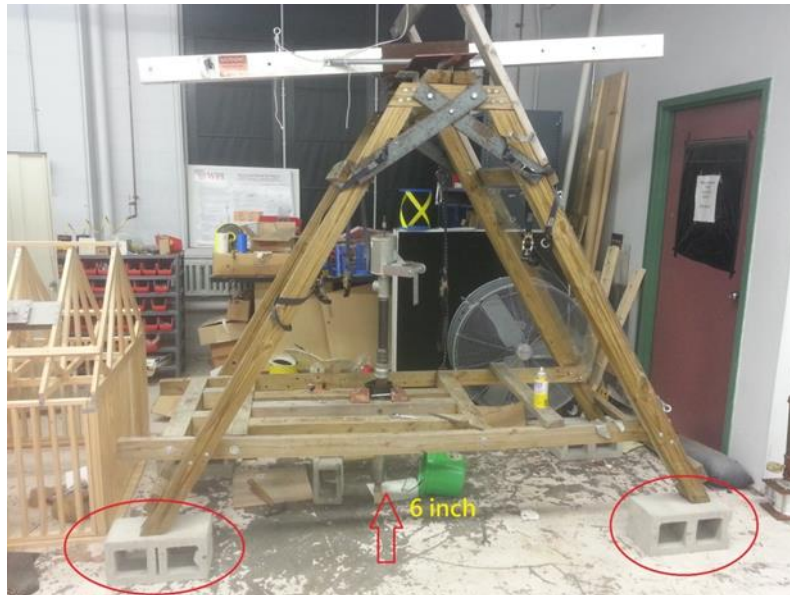


Figure 16 - Raised A-frame structure

- Extended the piping of the water-pump so that it may be lifted and able to pump water from the reservoir located beneath the system.

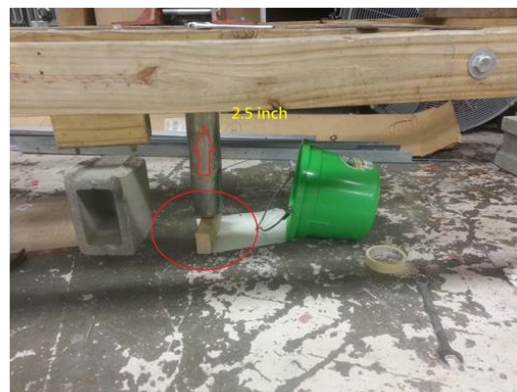


Figure 17 - Extended and raised water-pump piping

- Removed the wooden support beam, and raised it so as not to obstruct the lever-arm of the water-pump from having a full range of motion.



Figure 18 - Wooden support beam to be raised

Alterations were accomplished using simple tools supplied in the laboratory, as well as small number of screws and a wooden support beam that were purchased. After the purchase of the trailer, a water-reservoir was placed under the system to simulate a well. These adjustments made it possible to test the entire system in a wider variety of locations, allowing for a wider range of data sampling.

2.4.1 Water-dumping Mechanism

In order for the system to be efficient once placed on the trailer, there needed to be a constant supply of water. A water reservoir was placed on top of the trailer, under the A-frame, but for the volume of water being pumped to be measured the water could not simply be pumped directly back into the reservoir. The solution to this problem was the “tipping” bucket, which could be consistently filled with the same volume of water, and then emptied back into the reservoir beneath the system. The tipping bucket mechanism is pictured below:



Figure 19 – Inside of the tipping bucket mechanism

Two holes were drilled at one-third the height of the bucket from the bottom, and then a 3/8 inch rod was inserted through both holes. One hole was also drilled in the center of the bottom of the bucket, which was filled with a 3/8 inch screw. This allowed the bucket to hang underneath the outlet of the pump, and to tip along the axis of the rod.



Figure 20 - The weight underneath the tipping bucket

A weight was added to the bottom of the bucket to shift its center of mass downward, which allowed it to return upright after tilting to return the water into the reservoir. The weight used was in the form of an iron plate and hexagon knob, which attached to the screw placed in the bottom surface of the bucket.



Figure 21 - Completed tipping bucket mechanism

The points at which the horizontal rod rotates through wooden posts have extra space, allowing for easier rotation with less friction. The small screw protruding from the front of the bucket acts as a weight, causing the bucket to tip in that direction by being slightly heavier than the opposing. All modifications were made waterproof by using specialized glue. The tipping bucket mechanism allowed for a measurable method of returning water to the above-ground reservoir while field testing with the trailer system.

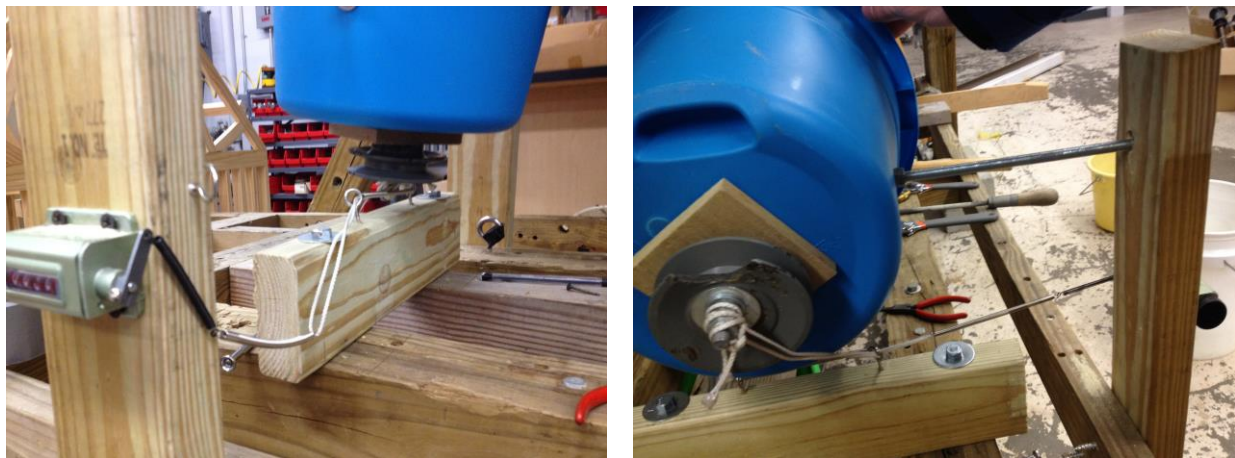


Figure 22 - Automatic-counter mechanism

An automatic counter was added for the most accurate, autonomous measurability possible. The images above depict how the bucket is attached to the counter, and then how the tipping of the bucket causes tension on the rope and pulls down on the lever-arm of the counter. Having the exact number of times the bucket as emptied water allowed the volume of pumped water to be more easily calculated. Approximately 6 liters of water are measured for each bucket dump.

2.5 MATLAB Simulation

In addition to observation of the pump system's performance during field testing and analysis of experimental data obtained, variation in performance parameters were evaluated based on a simulation of the system in MATLAB. This MATLAB simulation is a modification of code used in Olinger et al. (2013). The modification consisted of replacing the assumption of constant wind speed with a model based on power spectral analysis of horizontal wind speed to study the effects of wind speed variation on system performance. The power spectral density model used was from Van der Hoven (1956). This allowed comparison of performance parameters such as tether force and cumulative volume of water pumped for randomly varying wind speed compared to constant wind speeds.

This modified simulation allows not only for comparison with the previous simulation results but also comparison of experimental results with the goal of the periodic variation more accurately approximating the real wind conditions. Possible design modifications for the pump could then be considered in regards to trends observed in the simulations, such as the time varying kite tether force. Further experimentation after simulation was limited by weather in this project and suggestions are detailed in section 5.2.

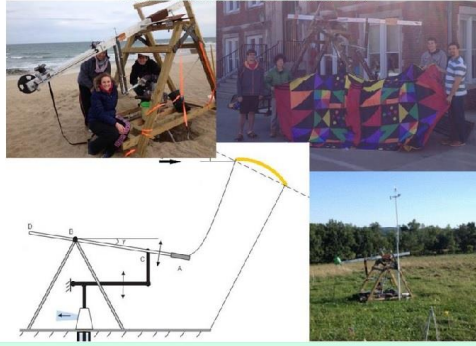
The existing MATLAB code simulates the forces and motion of the kite, tether, rocking arm, and pump over a user specified time interval by solving the four coupled differential equations of motion for the kite-tether-rocking arm system, using MATLAB®ODE23 solver on each time step in the interval (Olinger et al., 2013). Each time step also uses the four values from the solver, namely kite velocity, kite tether angle, rocking arm tip velocity, and rocking arm angle, to determine other useful quantities as a function of time such as tether force and pump displacement. Our study determines how these quantities are effected by allowing one user defined variable, namely wind speed, to vary with time. This varies the lift and drag forces on the kite and tether used in the differential equations.

2.6 Project Website

For this project to reach its maximum potential, the work needed to be publicized. A website describing and depicting past work and accomplishments had been created by an earlier MQP, but it had fallen out of date and was shut down. By reviving the webpage and bringing it up to date, the project concepts and ideas could be shared with the public.

To edit the webpage, which was in the form of a wiki-page, a specific markup language had to be learned. Once able to edit, the website was reorganized to begin at a welcome page with links to all other sections of the website. Section pages included current progress, images, and project components, with room to add more as the project progresses.

Welcome to the WPI Kite Power Wiki



Welcome

The WPI airborne wind energy (AWE) systems project in kite power is part of the ongoing research of WPI's Professor David Clinger, who is studying AWE systems and their potential uses. On this website, you will find descriptions of the past and present kite and water pump system, including any new modifications, goals, and a list of accomplishments to date. Be sure to check back in for updated photos, videos, and news!
We encourage you to visit the page explaining the [Current State of the research project!](#)

Objectives

The kite-powered airborne wind energy system is designed to be a cheap, renewable energy platform feasible in third-world or isolated applications.

- To create a method of extracting power from the wind
- To optimize the system, forming a reliable power system
- To minimize the cost of construction and maintenance
- To use a computer simulation to assist development

Navigation

- [Current State of the Project](#)
- [Development Timeline](#)
- [Virtual Animation](#)
- [Water Pump](#)
- [Power Generation System](#)

Full Scale Demonstration Videos

[The full YouTube video list can be found [here](#).]

Figure 23- Screenshot of the Welcome Screen on the Project Website

3.0 Results

3.1 Field Testing

The three stalling designs were tested in the Fall of 2013 in order to determine their effectiveness in powering the kite powered system. The main goal for the tests was to determine which method would stall and raise the rocking arm the most effectively, with data gathered to reinforce qualitative data gathered through observation. Ease of setup, range of effective wind speeds, performance during wind gusts, and durability were all taken into consideration while testing. The instrumentation was used to gather tension forces in one tether per test while simultaneously recording the rocking arm angle.

The trailing edge to ground configuration was tested without instrumentation. During testing, it was found that this method could raise and lower the rocking arm. The effectiveness of this method, however, was poor. The cycle was interrupted many times, creating a very low volume of water pumped. The method was easy to setup, however it required adjustment of the trailing edge tether once the kite was in the air, which required the kite to be brought back to the ground to adjust. The kite required wind speeds of about 10 miles per hour to fly, but once it was up there was no maintenance required as long as the average wind speed remained at this speed. During testing, gusts had a positive impact in the lifting power of the kite. From subsequent testing methods, however, gusts may be of concern as they caused the kite to crash into the ground several times. The durability of this method was a concern, particularly in the trailing edge tether connection method used on the kite. After moderate testing, the point where the loop created at the end of the trailing edge tether connected to the trailing edge line on the kite (which spanned between the two trailing edge corners) caused enough friction to weaken and eventually break the kite line. While this was easily mended with a knot, it ceased operation until the line was fixed.

The pulley configuration was tested with instrumentation during a very windy day. The effectiveness of this method was found to be marginally better than the trailing edge to ground configuration. Setup was the same as the trailing edge to ground method, only requiring one additional line to be connected. The wind ranges for operation were the same as the previous method. Performance during wind gusts was poor; the wind would pull the kite in a lateral direction, causing the arm to reach an angle above parallel with the ground and remain within a very small variation of there for the duration of the gust. This may have been caused by poor trailing edge tether length adjustment, but it was not tested adequately to determine. The durability problem discussed in the trailing edge to ground configuration occurred during testing of this method, but since both methods used the same trailing edge connection method, it applies to both. During the gusty testing day, the kite crashed into the ground, causing one of the fiberglass spars in the kite to eject out of its slot in the kite. This had to be mended and reinforced.

During the pulley configuration test, leading edge tether tension, trailing edge tether tension, minute-average wind speed, and wind gust speeds were measured.

Table 2- Pulley Configuration Test Data

	Leading Edge Tension (lbs)	Trailing Edge Tension (lbs)	Minute Average Wind Speed (mph)	Minute-Ranged Wind Gust Speed (mph)
Minimum	0.00	0.00	2.00	3.00
Maximum	150.86	18.33	18.00	22.00
Average	62.14	7.24	8.02	9.93
Standard Deviation	32.03	4.48	3.41	3.92

From this data it can be noted that the leading edge tension is far greater than the trailing edge tension. There is also great variation in the tension data, which is correlated to the variation in the average wind speed and further expanded by the higher gust speeds.

The leading edge stall configuration was tested for qualitative data without the opportunity to use instrumentation. This method provided the most cyclical motion of the kite, and a vast improvement in operation over the previous methods. The stall method created such a large impact in the lift of the kite that stall recovery became a concern. During testing, some stalls became so severe that the kite folded in the air, causing the kite to fall to the ground without any chance of in-air recovery. Additional modifications were required to be made to the kite for this method, causing additional initial setup time, but similar subsequent setup times as the previous methods. In order to remain airborne, the kite required the same average wind speed as the previous methods, however in order to recover from a stall, higher wind speeds were desired. Gust performance was similar to average wind speed performance, however more data is required. The kite durability for this method appeared to be an improvement over previous methods, with the largest concern being in the modifications made to accommodate the stalling tether. No severe crashes were observed similar to the one that caused the fiberglass rod ejection, however more testing is required.

3.2 MATLAB Simulation

The power spectral density for horizontal wind speed that was used to model varying wind speed with in the simulation is depicted in Figure 24 below (Van der Hoven, 1956). Twenty points on the specific kinetic energy vs. frequency curve are used as samples at an interval of 50 cycles per hour to obtain a time series for horizontal velocity (as it is the square root of specific kinetic energy). A discrete inverse Fourier transform generates the time series for horizontal velocity in a MATLAB script separate from the simulation loop to save time on computation.

There are two main peaks in specific kinetic energy at 0.001 cycles per hour and 60 cycles per hour. Points across the entire frequency domain are used in the generation of the times series for wind velocity for completeness, however on the short simulation interval only partials with high frequencies have periods small enough to be visible in the results. These frequencies are also of interest because they are close to the desired frequency of the lift-stall cycle and their peaks at distinct points within the simulation interval can be directly compared with other simulated parameters at those points in time.

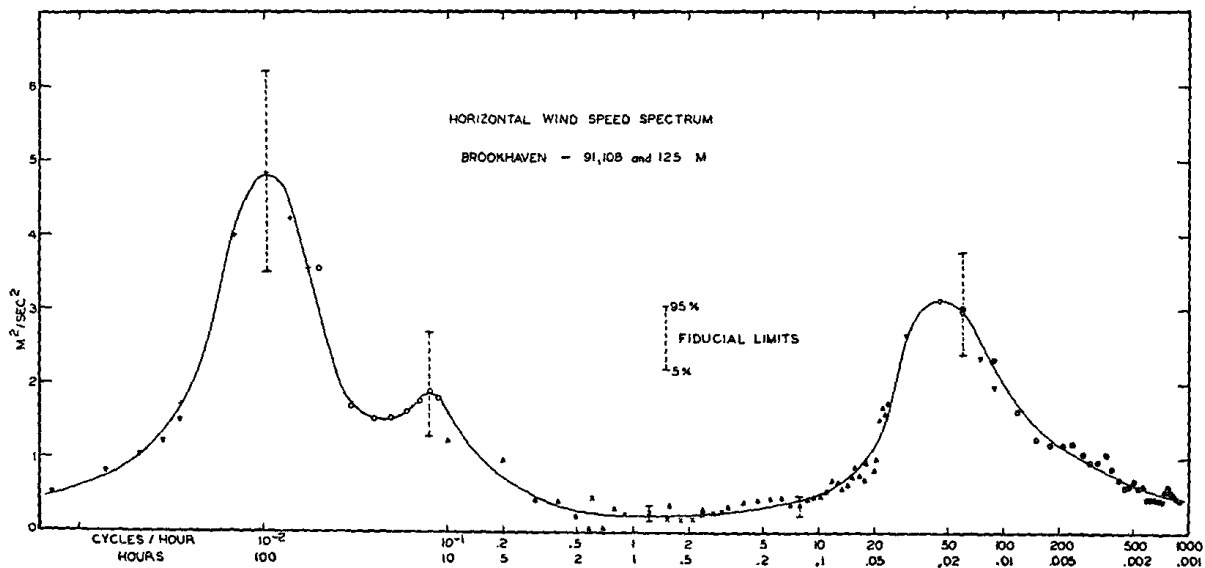


Figure 24 - Power Spectral Density of Horizontal Wind Speed (Van der Hoven, 1956)

The primary figure of merit in the pump systems performance is the total volume of water pumped during the simulation interval. For the original simulation on a 20 second interval with a constant wind speed of 6 meters per second as reported in (Olinger et al., 2013), the total volume of water is 3.23 liters. With the wind speed oscillating around this average speed of 6 meters per second with relative deviations from the mean proportional to the deviations at each frequency in the power spectral density model, the total volume of water pumped on a 20 second interval drops to 2.16 liters. This is approximately 66% total volume efficiency of the idealized model. Additionally, there is a small decrease in average tether tension from 458N to 445N. The results are shown in the figures below.

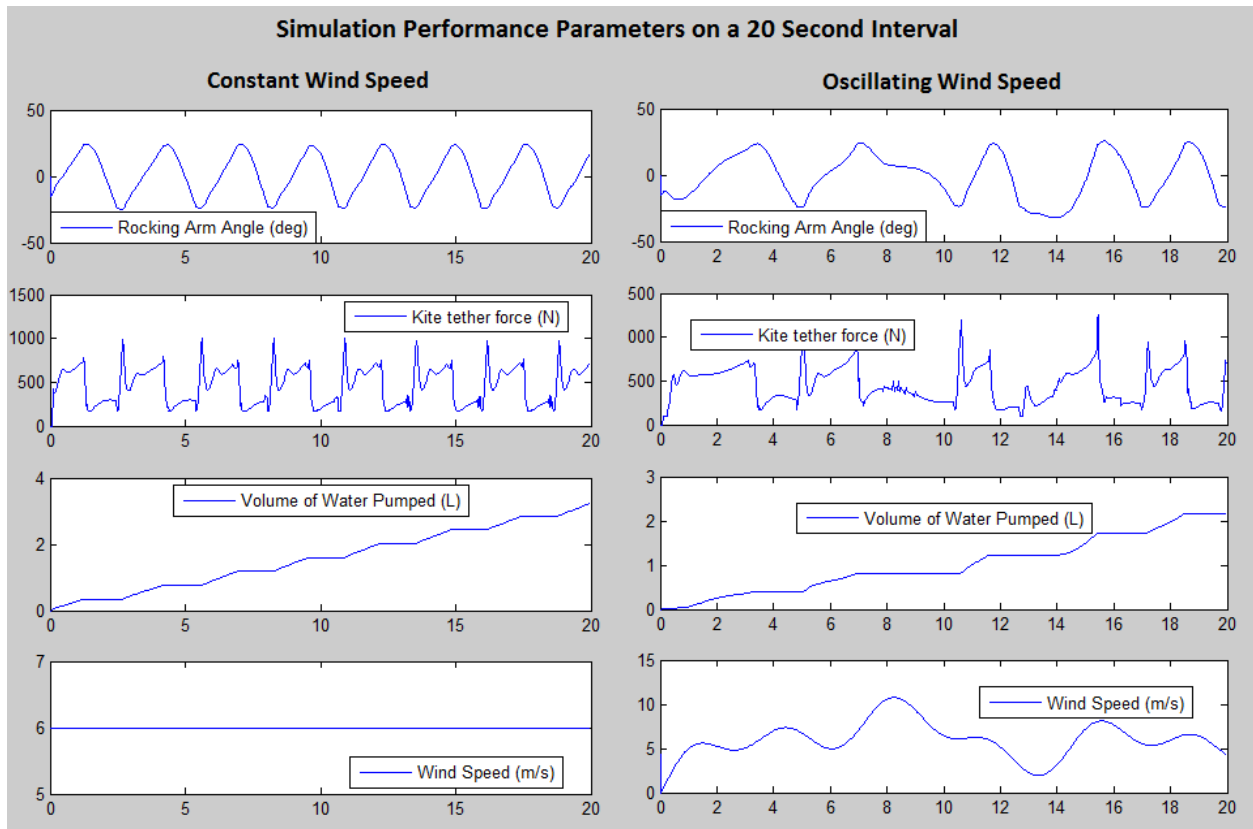


Figure 25 - Simulation Performance Parameters on a 20 Second Interval

The angular velocity of the rocking arm is the variable in the set of differential equations solved by the simulation that dictates pump piston displacement over time, which is proportional to the total volume of water pumped on the interval. The simulation with varying wind speed shows a decrease in average angular velocity of the rocking arm from 0.87 degrees per second to -1.22 degrees per second. Although the mean and extreme values of the tether force are similar in each case, there are longer time intervals of maximum tether force where the kite and rocking arm are ascending (power stroke). This is what causes a decrease in mechanical power of the rocking arm system shown by the decrease of angular velocity, while force (and thus torque) remains constant. The power decrease then manifests itself in the smaller volume of water (less work done by the pump). The above relations are shown in the figures below.

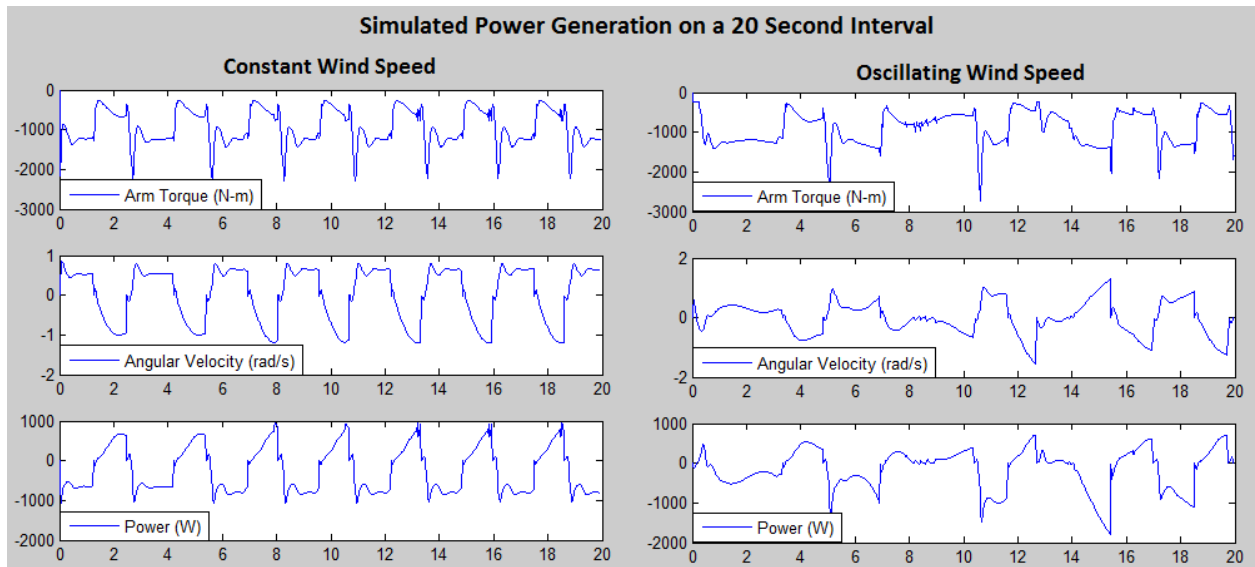


Figure 26 - Simulated Power Generation on a 20 Second Interval

4.0 Summary and Conclusions

The following are the primary accomplishments of this project:

- Performed further field testing on the kite system to gather data including tether tension, arm angle, and water pumping rates
- Created a functioning VI in LabVIEW to gather data from testing instrumentation
- Proposed and implemented mechanical modifications to further improve the function of the water pump and power generation system based on the measured data
- Modified an existing simulation of the water pump to model wind gusts and random wind conditions using MATLAB
- Designed and tested additional kite stalling mechanisms
- Designed and implemented a portable trailer system and automated pumping volume measurement system in order to transport the water pump and improve field testing

Each of the goals established in the beginning of this project were accomplished. Given that field testing is weather dependent, the newly designed stalling mechanisms and trailer system were not able to be extensively tested. Due to this lack of testing, sufficient amounts of testing data were not collected and analyzed to gauge efficiency, providing groundwork for future projects.

5.0 Recommendations and Future Work

Following the progress of this project, there are areas in which work needs to be continued. This section details recommendations based on the experience of this WPI MQP project.

5.1 Trailer Field Testing

With the trailer system in place, field testing can take place in a number of new locations. Testing in a wider variety of locations can improve the frequency, and the quality, of gathered data. A more diverse sample size of testing sites will better represent the varying conditions under which the wind-powered water pump system will be expected to operate. This new data will lead to more representative data, and eventually to an optimal system.

5.2 Leading Edge Stall Recovery System

When using the leading edge stall method, some stalls can be too severe for the kite to recover from. This could be fixed by adding a rigid member to the kite spanning the width of the kite, causing the kite to expand to the full breadth when the stalling force is released.

5.3 Kite Auto-Launch

Developing an automatic launching method for the kite is crucial in achieving the most efficient operation of the water pump system. If this system is to be used in developing nations, it needs to operate such that a person will not need to re-launch the kite every time the wind diminishes. Possible structural changes include a flexible rod along the width of the kite to keep the leading edge raised off the ground with the flow cells open while the kite is landed, or a solid frame that includes two legs on the leading edge connected to a rod running to the trailing edge of the kite. One potential auto-launch design is shown below in Figure 26:

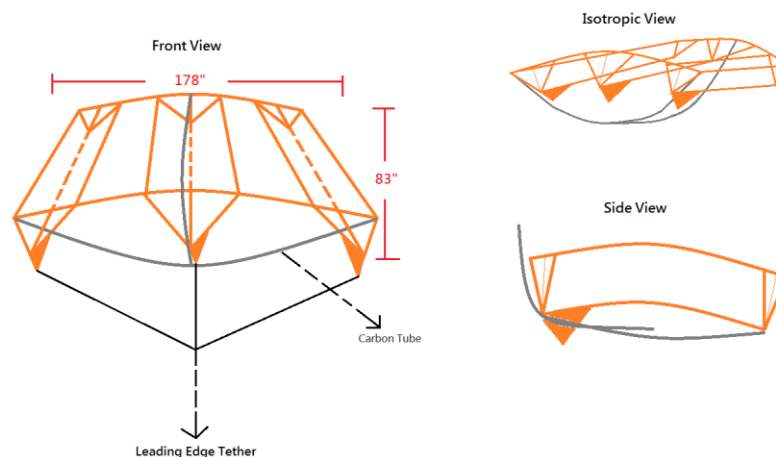


Figure 27 - Auto-launch concept design

5.4 Website Updates

Continuously updating the website will increase public awareness of this project and its research. If the information on the web page is kept up to date, it will portray the kite-powered water pump system as positive and progressive, which can be very beneficial. If this new, upcoming concept is positively received by the public then it will increase the likelihood of its use.

5.5 Instrumentation Housing

The instrumentation is currently in an exposed state, particularly the DAQ and the amplifier. When moving or packing and unpacking the instrumentation, stresses are applied to the wires that are connected to the amplifier and the DAQ. This causes wires to often be pulled from their slots and sometimes damaged. There are also bits of wire that are exposed to the elements and may cause problems in testing. A housing may be constructed which will better protect the wiring and instrumentation as well as possibly reducing setup and breakdown times.

6.0 References

- Bartosik, Kyle, Jennifer Gill, Andrew Lybarger, Daniel Nyren, John Wilder. "Design of a Kite-Powered Water Pump and Airborne Wind Turbine." (2012). Web. 1 April 2014 <<http://www.wpi.edu/Pubs/E-project/Available/E-project-042512-193217/>>.
- Butler, Valerie, Jeffrey Corado, Kimberly Joback, Bryan Karsky, Matthew Melia, Robert Monteith, and Brandy Warner. "Re-Design of the WPI Kite-Powered Water Pump and Wind Turbine Systems." (2013): n. page. Web. 11 Oct. 2013. <<http://www.wpi.edu/Pubs/E-project/Available/E-project-042513-003509/>>.
- Chretien, Larry, Michele Bilodeau, and Kelly Muellman. *Feasibility Study Report For Wind Power at Overlook Farm*. Mass Energy, 2008. Print.
- Diehl, Moritz. *Airborne Wind Energy*. 1st ed. Berlin: Springer Berlin Heidelberg, 2013. 3-22. Print.
- Loyd, M., "Crosswind Kite Power," *Journal of Energy*, Vol 9, No. 3, 106-111, 1980.
- Mackay, D.: *Sustainable Energy- Without the Hot Air*. UIT Cambridge, Cambridge (2009)
- Olinger, David J., "Integrated Study of Ground Tethered Energy Systems, Proposal to NSF Energy for Sustainability Program, 2010.
- Olinger, David J., Jitendra S. Goela, and Gretar Tryggvason. "Modeling and Testing of a Kite-Powered Water Pump." *Airborne Wind Energy*. Part IV.10.1007/978-3-642-39965-7_22 (2013): 387-401. Print.
- "Through Hole Donut Load Cell Compression Only (1.50 O.D.)." *Transducer Techniques*. N.p., n.d. Web. 22 Apr. 2014. <<http://www.transducertechniques.com/thb-load-cell.aspx>>.
- United States. National Aeronautics and Space Administration. *NASA Surface meteorology and Solar Energy (SSE) Release 5 Data Set*. 2005. Web. <https://eosweb.larc.nasa.gov/sse/global/text/10yr_wspd50m>.
- Van der Hoven, Isaac. "Power Spectrum of Horizontal Wind Speed in the Frequency Range from 0.0007 to 900 Cycles per Hour." *Journal of Meteorology* 14: 160-164. Print.
- WAsP, 2006. *The Wind Atlas Analysis and Application Program*. <<http://www.WAsP.dk>>.

Appendix A. Instrumentation Manual

Load Cell

The load cell has four different wires coming from the unit that are housed in a single grey shield casing. The wires are assigned as:

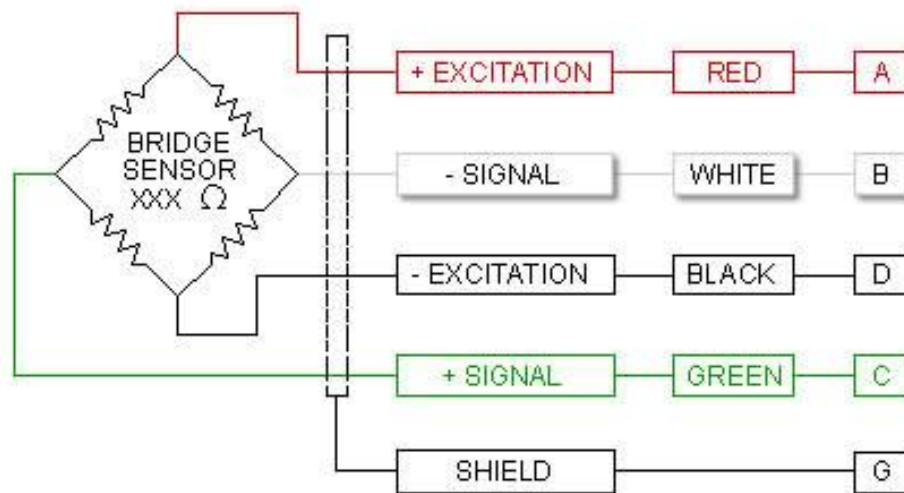


Figure 28- Wiring Diagram for THB-1K-S Load Cell (Transducer Techniques)

The red and black wires are the excitation, or power, wires. The load cell requires 10 volts of DC current. This is measured as a 10V increase compared to the black wire. The green and white wires are the signal wires, which output a voltage when a compressive load is applied to the cell. This voltage is read as a differential between the green and white wires, then amplified and scaled to the known load.

Inclinometer

The inclinometer has 3 wires: red, white, and blue. The red wire is the +5V DC wire, the white is the signal output, and the blue is the ground wire. These are connected to an extension wire used to bridge the gap between the DAQ and the rocking arm where the inclinometer is housed. The red and white inclinometer wires are connected using clips to the red and white extension wires to retain consistency. The blue inclinometer wire is connected to the green extension wire.

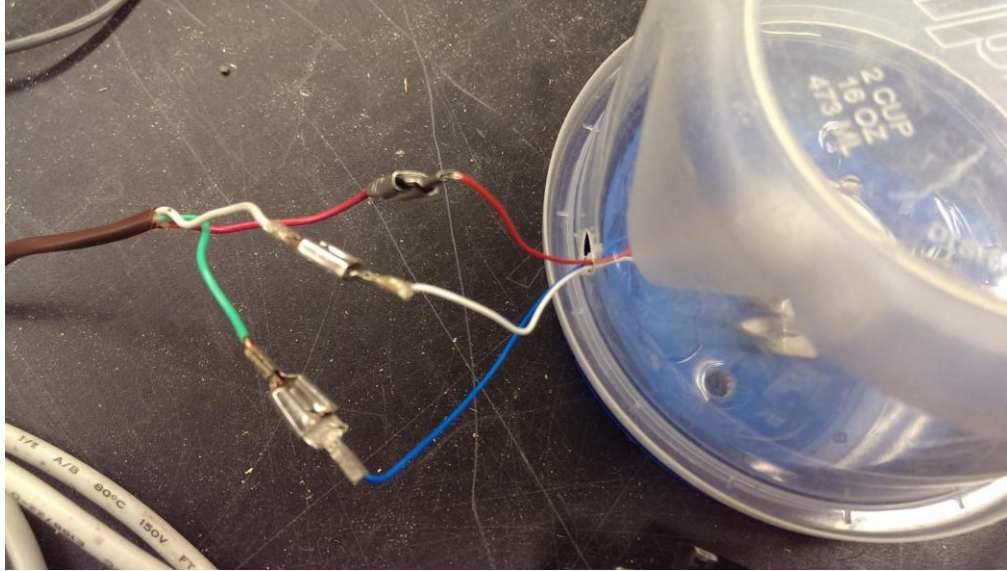


Figure 29- Inclinometer Extension Wiring

Battery

The battery is rated at 12V and used to power the amplifier. It is connected to the amplifier by 2 connectors often used for 9V batteries. The wires are connected to the top of the battery according to the visible polarity, however due to the nature of the connection, the wires leading into the amplifier are put in backwards, the black wire to the positive terminal and the red to the negative terminal.

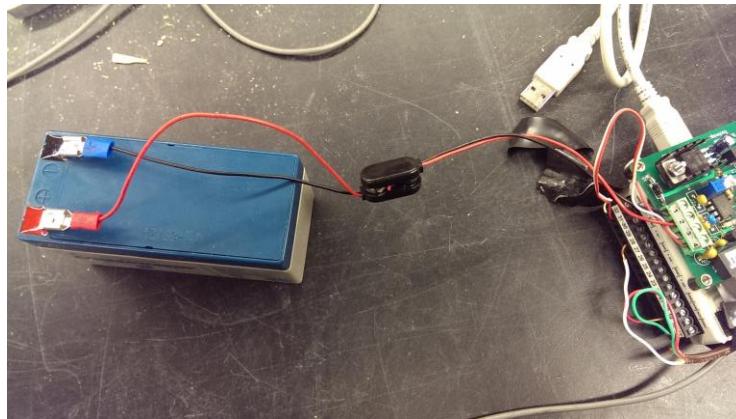


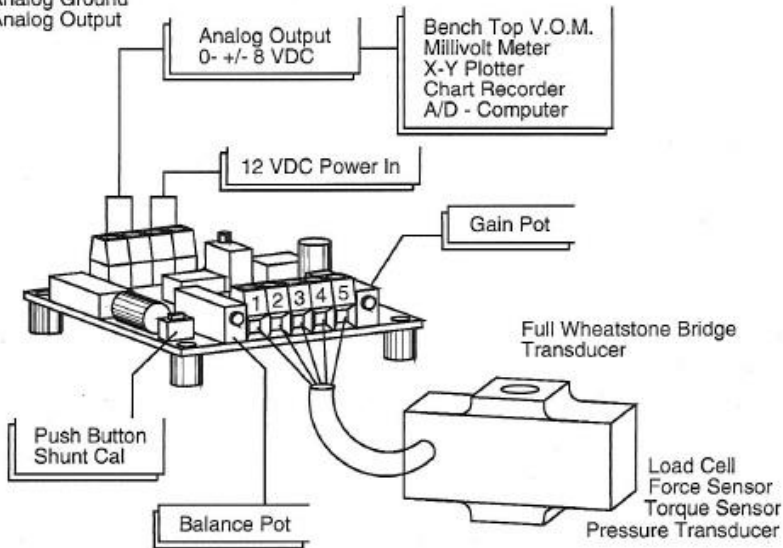
Figure 30- Battery Wired to Amplifier

Amplifier

The amplifier used has two terminal blocks on either side of the unit. One block has 5 connection ports and is used to receive the signal to be amplified. The other block has 4 connection ports which are used to power the amplifier and to transmit the amplified signal to the DAQ.

**Power Supply / Analog Output
4 Pin Terminal Block**

- 1: + 12 VDC
- 2: Power Ground
- 3: Analog Ground
- 4: Analog Output



**Transducer Input
5 Pin Terminal Block**

TM0-1	Transducer
1	+ Excitation (Red)
2	- Signal (White)
3	+ Signal (Green)
4	- Excitation (Black)
5	+ Shield

Figure 31- Amplifier Wiring Diagram

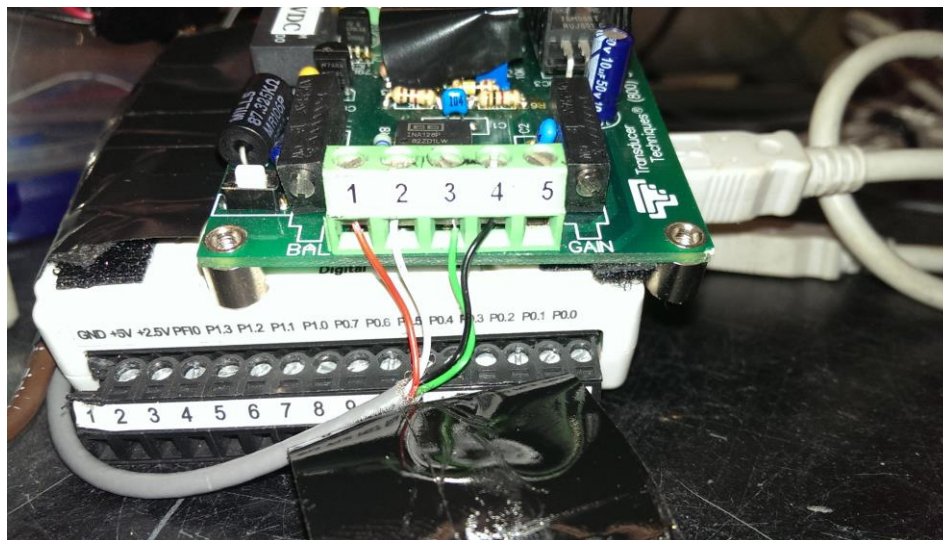


Figure 32- Load Cell Wired into Amplifier

The input of the load cell wires is shown above. The wires are plugged according to the comparison of figure 23 and figure 25. It is important to note that the wiring diagram for the load cell lines up directly with the wiring diagram for the amplifier, with no differences in color or function in the wires. The “5” slot is left empty as there is no shield wire.

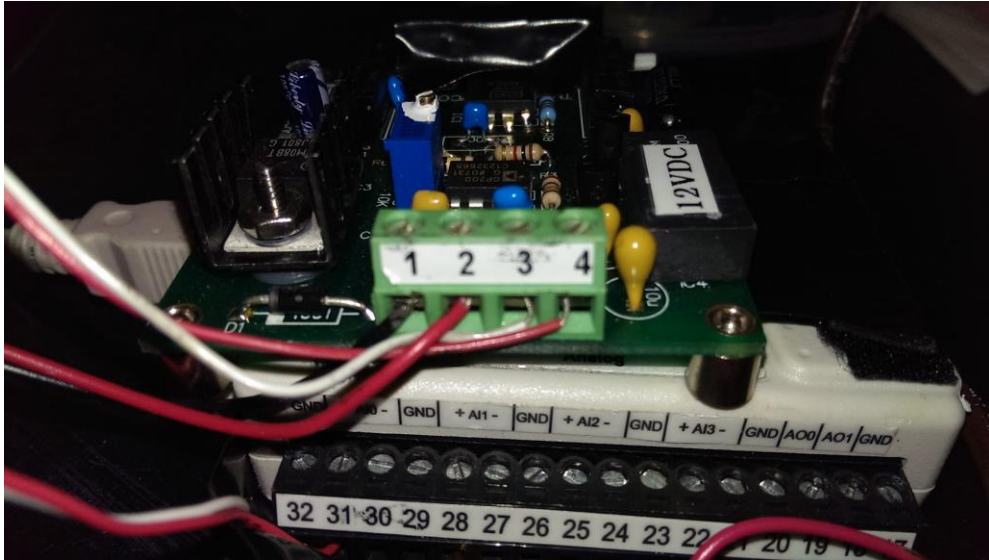


Figure 33- Power and Signal Output Wired from Amplifier

The 4 port block uses the “1” and “2” ports for power. The “1” port is the positive port as indicated in figure 23, however because of the reversal in the polarity due to the battery connection wires, the black “positive” wire is plugged into the “1” slot and the red “negative” wire is plugged into the “2” slot. The “3” slot is used for a reference ground for the output signal. The “4” slot is used for the amplified analog signal output.

DAQ

The DAQ is the device used to power the inclinometer and receive and interpret the signals output by the amplifier and inclinometer. The instruments used only transmit analog signals, and thus the side of the amplifier labeled with slots “17” through “32” is used. The other side of the amplifier uses digital input and output.

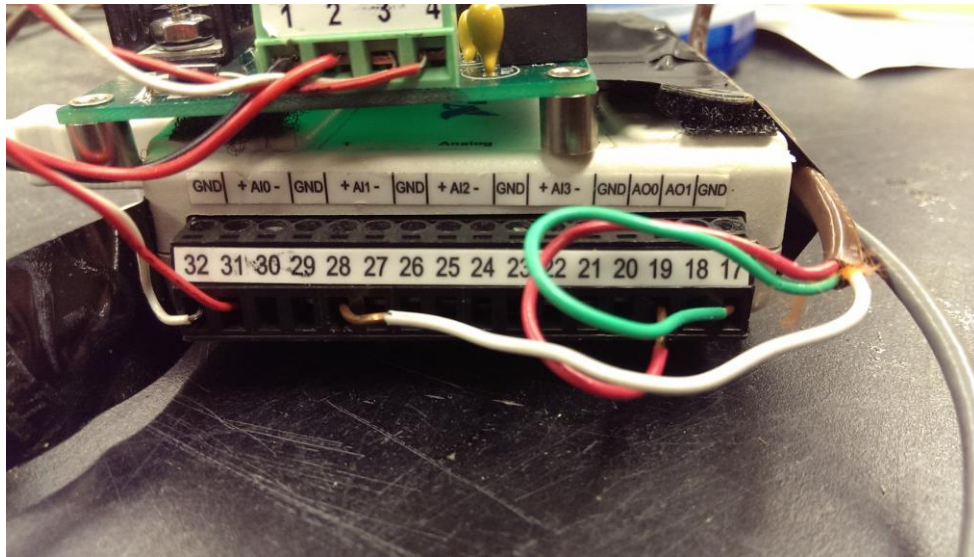


Figure 34- DAQ Wiring

The DAQ is wired to receive the signals from the amplifier in “AI0” and the inclinometer in “AI1.” The amplifier puts out an analog signal on the red wire from the “4” slot on the 4 terminal block. This is wired to slot “31” on the DAQ, also labeled as “+AI0.” The white wire used to measure the differential voltage wired from the “3” slot in the 4 terminal block on the amplifier is plugged into the ground (GND) in slot “32” on the DAQ. Together these allow the DAQ to measure the signal output from the amplifier for the load cell. The inclinometer is powered by the DAQ while also transmitting the signal to it, allowing the instrument to operate without the amplifier. The white signal wire is plugged into the “28” “+AI1” slot. The red excitation wire is plugged into the “19” “AO0” which is used for analog signal output and configured to output 5V DC. The final green ground wire is plugged into “17” “GND” slot.

Wiring Overview Table

Table 3 - Wiring Overview

Device	Wire	Purpose	Destination	Notes
Battery	Black	+12V DC	Amplifier 4 terminal block slot 1	Black wire after the polarities have been switched at the separable junction.
	Red	Excitation Ground	Amplifier 4 terminal block slot 2	Red wire after the polarities have been switched at the separable junction.
Load Cell	Red	+10V DC	Amplifier 5 terminal block slot 1	
	White	- Signal	Amplifier 5 terminal block slot 2	
	Green	+ Signal	Amplifier 5 terminal block slot 3	
	Black	Excitation Ground	Amplifier 5 terminal block slot 4	
Inclinometer	Red	+5V DC	DAQ AO1 slot 19	
	White	Signal	DAQ AI1 slot 28	
	Green	Ground	DAQ GND slot 17	
Amplifier	White 4 terminal block slot 3	Reference Ground for Signal Output	DAQ GND slot 32	Amplified Load Cell Signal
	Red 4 terminal block slot 4	Signal Output	DAQ AI0 slot 31	Amplified Load Cell Signal

LabVIEW Virtual Instrument

The LabVIEW VI is constructed to be able to operate a load cell, an inclinometer, a torque meter, and a tachometer. In this project, only the load cell and inclinometer were used.

The first step in setting up the VI is to go to the block diagram and locate the AI Voltage item. From the “physical channels” input on this node, create an “indicator” and switch back to the front panel. Using this new indicator, figure out which device the DAQ is and note the name (Dev0, Dev1, etc.) and channels (ai0, ai1, etc.) being used. Return to the block diagram and delete the indicator that was just created and replace it with a constant input. In this constant, type in the device and channels that are to be read by the DAQ. An example is shown below:

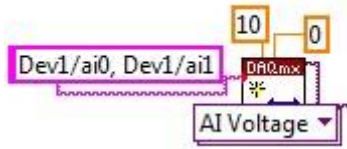


Figure 35- Sample Device/Channel Input for LabVIEW VI

In this example, two channels on one device are being used. The VI is configured to have the ai0 channel output to the load cell display, the ai1 channel output to the inclinometer display, the ai2 channel output to the torque meter display, and the ai3 channel output to the tachometer display. These channels must be consistent with the DAQ wiring.

On the front panel, there are input boxes on the left that are used to calibrate the load cell and inclinometer. On the left of the front panel, there is a grouping of items that looks like figure 33.

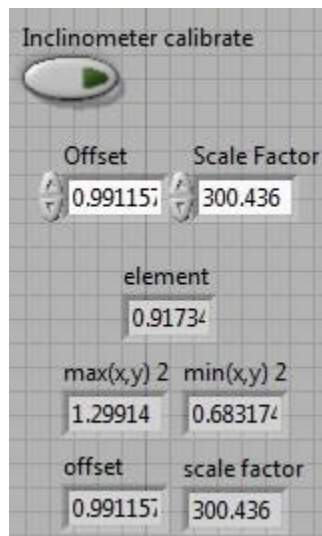


Figure 36- Inclinometer Calibration Tools

This is the visual input and output for a program that calibrates the inclinometer. To operate the program, begin by clicking the “Inclinometer calibrate” button. Then, hold the inclinometer so that the text on the front of the instrument is parallel with the ground. Rotate the inclinometer to +90 degrees and then to -90 degrees several times until the output that is visible on the inclinometer graph on the front panel mirrors the movement of the instrument. When the graph and rotation of the instrument are the same, copy the values from the “offset” and “scale factor” blocks at the bottom of this grouping into the “offset” and “scale factor” blocks near the top. These top values become permanent. With these permanent values in place, the “Inclinometer calibrate” button can be pressed again to terminate the calibration program.

Calibration of the load cell is done manually using the calibration tools on the front panel located just below the inclinometer calibration group.

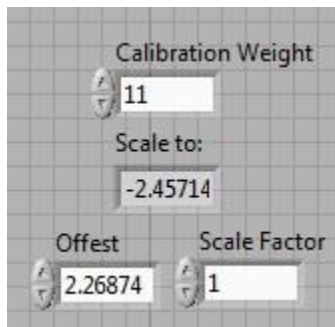


Figure 37- Load Cell Calibration Tools

The load cell is calibrated using a known load. First, begin by entering the calibration weight (known load) in the units that are desired for the output on the graph. Next, set the “Offset” to 0 and the “Scale Factor” to 1. Run the VI and note the value that the load cell is outputting on the graph while there is no load on the load cell. This value is the value that must be placed into the “Offset” value. After putting this offset value in, the graph should output a value very near 0. Place the known load on the load cell. A value will appear in the “Scale to:” output box, which must be copied into the “Scale Factor” box. The load cell is now calibrated. In order to check accuracy, another known load may be weighed and compared to the output on the graph.